Available online at www.sciencedirect.com
SCIENCE DIRECT®
Journal of Molecular Catalysis A: Chemical 213 (2004) 199–205
JOURNAL OF MOLECULAR CATALYSIS A: CHEMICAL
www.elsevier.com/locate/molcata

The effect of secondary metal on Mo_2C/Al_2O_3 catalyst for the partial oxidation of methane to syngas

Quanli Zhu*, Bin Zhang, Jun Zhao, Shengfu Ji[1], Jian Yang, Jiaxin Wang, Hanqing Wang

State Key Laboratory for Oxo Synthesis and Selective Oxidation, Lanzhou Institute of Chemical Physics, Chinese Academy of Sciences, Lanzhou 730000, PR China

Received 24 March 2003; received in revised form 18 June 2003; accepted 18 June 2003

Abstract

Investigation on molybdenum carbide catalyst, its oxide precursor and its modifiers was performed using temperature programmed surface reaction (TPSR) technique, BET surface specific area and X-ray diffraction (XRD) measurement. The carbide catalyst and its modifiers were evaluated using microreactor apparatus. The evaluation result showed that the addition of nickel promoted the POM to syngas, the addition of copper exhibited weaker promotion at the initial stage, but it turned unfavorable to the POM to syngas hereafter. As for potassium doped catalyst, it was unfavorable to the POM. According to the characterizations, the effect of added metals on the carburization, especially under the condition of POM, was elucidated.

Keywords: Carbide catalyst; Promotion; TPSR; XRD; BET

1. Introduction

The possibility to use early transition metal carbide as a catalyst for the methane conversion, such as the partial oxidation of methane (POM) to syngas, methanol, formaldehyde and dehydrogenation of methane to benzene, etc. has been investigated recently [1–10]. Although noble metals as a catalyst are effective for these reactions, these carbides, especially of molybdenum or tungsten, have attracted a great deal of attention due to their unique properities. According to the results by Green and his coworkers [1–4], Mo_2C or WC showed the activity high enough to be be similar to that of noble metal catalyst for the partial oxidation of methane to syngas at elevated pressure and temperature. However, at ambient pressure, they all deactivated rapidly due to the transformation of carbide into MO_2. This phenomenon indicates that the carbide is unstable under the existence of oxygen species. This instability of molybdenum carbide was also affirmed by others experiments [5–8].

We have evaluated a series of supported molybdenum carbide catalyst doped with different secondary metals for the POM to syngas, for the purpose of its improvement of catalytic stability. It was found that the addition of nickel promoted the conversion of methane to syngas, and that the addition of potassium prevented the conversion of methane and the selectivity toward CO or H_2. While the addition of copper showed promotion at initial stage, and then this promotion turned the reversed. It is surprising that 0.5 wt.% content of Ni can significantly improve the methane conversion and selectivity toward CO or H_2, in particularly, the stability, though nickel is highly active for the POM to syngas. In order to investigate the effect of these secondary metals on the surface properties of molybdenum carbide, the temperature programmed surface reaction (TPSR) measurements, as well as other characterization technique, were carried out. The result is presented in the paper, wherein the effect of the secondary metals is elucidated.

2. Experimental

2.1. Sample preparation

Molybdenum trioxide was obtained from ammonium heptamolybdate (AR) heated at 773 K for 3 h.

* Corresponding author. Tel.: +86-931-8278319; fax: +86-931-8277088.
E-mail addresses: qlzhu0001@sina.com (Q. Zhu), jisf@mail.buct.edu.cn (S. Ji).
[1] Co-corresponding author.

1381-1169/$ – see front matter © 2003 Elsevier B.V. All rights reserved.
doi:10.1016/j.molcata.2003.06.001

Alumina-supported molybdenum trioxide sample was prepared using alumina (BET surface area, 303 m^2/g, Research Institute of Lanzhou Chemical Industry Corporation, Lanzhou, P.R. China) impregnated in the solution of ammonium heptamolybdate and ammonia (AR) with calculated amount of molybdenum. Then, under the stirring, the mixture solution was evaporated to dry in water bath (353–363 K). The obtained powder was transferred into oven (383 K) for 12 h, and it was calcined at 773 K for 4 h. The doped sample was prepared using the above alumina-supported sample (before calcination) impregnated with solution of calculated amount of nickel nitrate (AR), copper nitrate (AR) or potassium hydroxide (AR), and then calcined at 773 K for 4 h after it was dried at 383 K for 12 h.

The samples used for evaluation was carburized according to procedures similar to those described in reference [11]. Sample (0.15 g) loaded in a quartz tube equipped with coarse quartz fibre at central part was carburized with 20 vol.% methane in hydrogen (all high purity, 1.47 mol/min) at ambient pressure. Temperature increases at ramped rate of 10 K/min from room temperature to 573 K, then 1 K/min from 573 to 1123 K. It was maintained at last temperature for 2 h and then treated with hydrogen (1.18 mol/min) in order to remove the deposited carbon. The passivated sample was obtained from the just carburized sample cooled in helium to room temperature and then passivated with 1 vol.% oxygen in helium (all high purity) for 12 h before contact with air.

2.2. Catalyst evaluation

Catalysts were evaluated in situ in a continuous flow reaction system with fixed catalyst bed using methane and oxygen as feedstock at ambient pressure, after it was just carburized and pretreated with hydrogen. Products were analyzed using gas chromatograph fitted with thermal conductivity detector. The separation of products was achieved using Porapak Q and 5 A zeolite packed columns, with helium as carrier gas. The calculation of conversion and selectivity was carried out according to the equations described elsewhere [3].

2.3. Catalyst characterization

TPSR measurements were carried out using catalytic microreactor (AMI-100, Altamira Instrument, USA), usually loaded with 0.15 g of sample, and the products were detected with quadrupole mass spectrometer (Ametek Instruments, Dycor system 1000). Sample was pretreated with helium at flowing rate of 30 ml/min, heated at rate of 10 K/min from room temperature to 773 K, and it was maintained at 773 K for half an hour. When it was cooled in helium to the temperature below 473 K, helium was shifted to methane and the gas flowing rate was controlled with mass flowmeter at 30 ml/min. Then, TPSR experiment was to begin with temperature ramped at rate of 10 K/min from 473 to 1123 K.

The specific surface areas of the passivated samples were measured on an ASAP 2010 (Micrometrics Instrument Corp.) using the N_2 adsorption method. The crystalline components of the materials were identified by X-ray diffraction (XRD) using a D/max-RB model X-ray diffractometer with Cu Kα radiation ($\lambda = 0.15418$ nm).

3. Results

3.1. Catalyst evaluation

The evaluation results of different catalysts are shown in Figs. 1 and 2. It can be found that the nickel doped carbide catalyst for the POM to syngas exhibited the highest methane conversion (96%, Fig. 1). Under the same condition, the methane conversion over Ni/Al_2O_3 decreased from 60% at beginning rapidly to ca. 37% after 1.5 h, while over the Mo_2C/Al_2O_3, it decreased from 84 to 43%. As for potassium doped catalyst, the methane conversion dropped from 62 to 31% after 1.5 h run. For copper doped catalyst, methane conversion decreased from ca.74 to 50%, but, this decrease was slower at initial stage (for about 1 h), rapider hereafter.

As shown in Fig. 2, the selectivity to CO (S_{CO}) or to H_2 (S_H) is highest (ca. 96%) and most stable over nickel doped catalyst. For Mo_2C/Al_2O_3 catalyst, S_{CO} went up from ca. 21% at beginning to 64%, while S_H was more stable than S_{CO}, almost maintained at ca., 61.5%. As for copper doped catalyst, S_{CO} and S_H were relatively stable at initial stage, but S_H (70%) was a little lower than S_{CO} (73%). After the initial period, S_H or S_{CO} decreased with time. S_H or S_{CO} over potassium doped catalyst was the lowest, ca. 41%, respectively, at 45 min, and they showed different directions with time, augmenting to some extent for S_H, declining a little for S_{CO}.

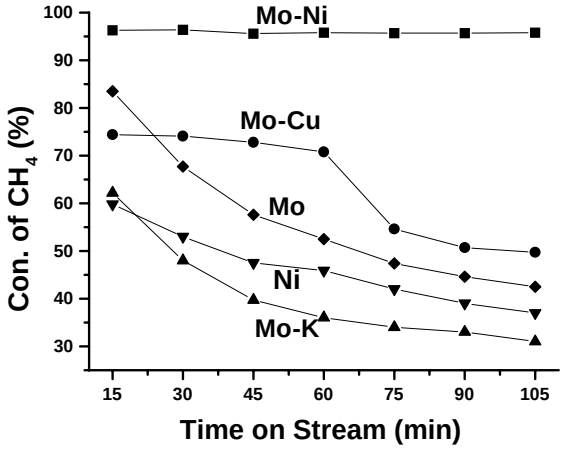

Fig. 1. Conversion of methane vs. time on stream (reaction conditions: 1123 K; ambient pressure, CH_4:O_2 = 2.05 : 1, GHSV = 2×10^5 ml/h g catalyst. Mo–Ni, 0.5% Ni, 35.4% Mo_2C/Al_2O_3; Mo–Cu, 1.4% Cu 35.4% Mo_2C/Al_2O_3; Mo, 35.4% Mo_2C/Al_2O_3, Ni, 0.5% Ni/Al_2O_3; Mo–K, 1.2% K 35.4% Mo_2C/Al_2O_3; mass ratio %).

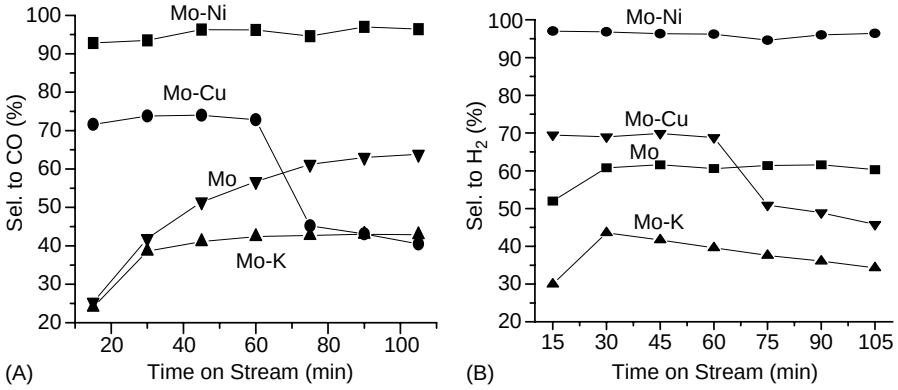

Fig. 2. Selectivity vs. time on stream (A) S_{CO}; (B) S_H; legends same as in Fig. 1).

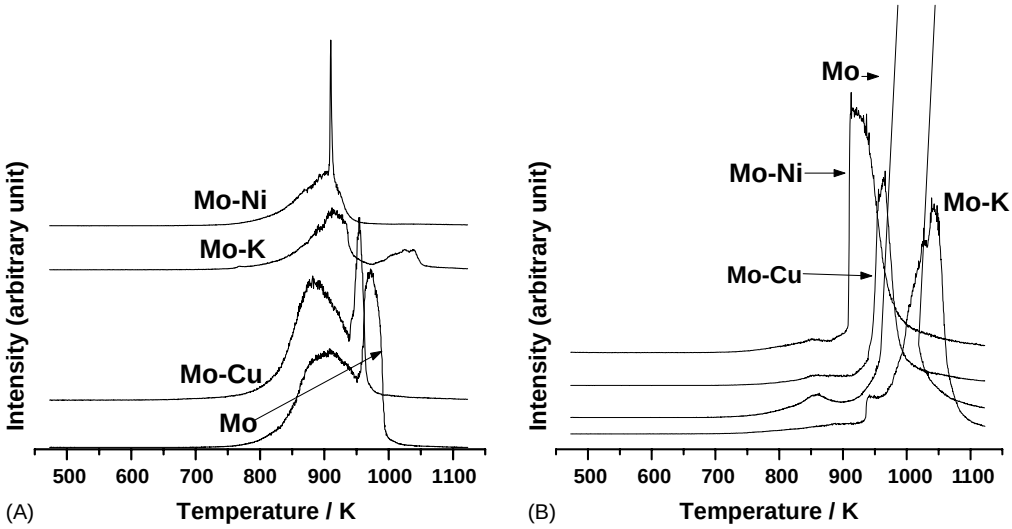

Fig. 3. Products formation during CH_4–TPSR (A) CO_2; (B) CO. Mo, 50% MoO_3/Al_2O_3; Mo–Cu, 1.2% CuO 50% MoO_3/Al_2O_3; Mo–K, 1.0% K_2O 50% MoO_3/Al_2O_3; Mo–Ni, 0.5% NiO 50% MoO_3/Al_2O_3; mass ratio %).

3.2. Characterization by CH_4–TPSR

The patterns of CH_4–TPSR are given in Figs. 3–5. As shown in Fig. 3A, there were two peaks, one at ca. 906 K and the other at 973 K, of CO_2 formation during the CH_4–TPSR for the MoO_3/Al_2O_3 (Mo) sample. For the copper doped sample (Mo–Cu), the two peaks shifted to 883 and 954 K, respectively, while the two peaks shifted to 912 and ca. 1038 K, respectively, for the potassium doped sample (Mo–K). As

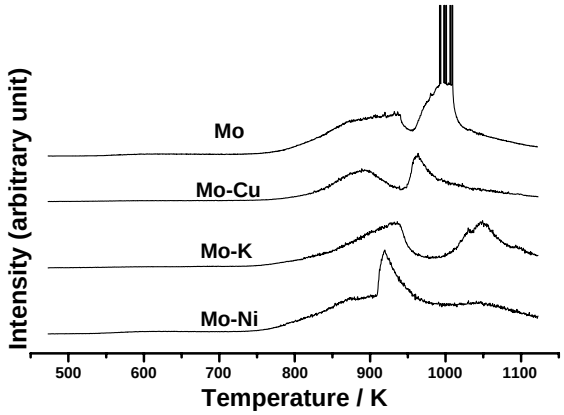

Fig. 4. Water formation during CH_4–TPSR (legends same as in Fig. 3).

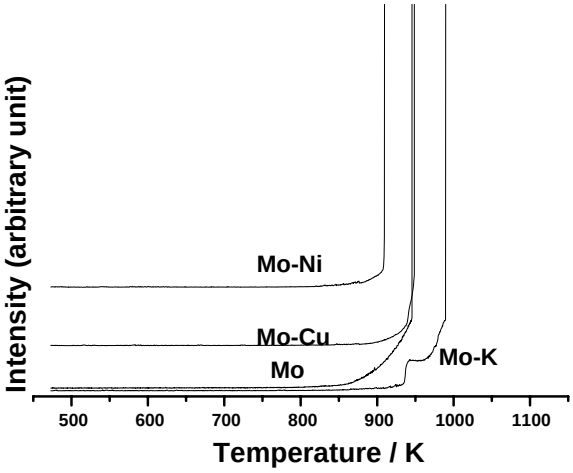

Fig. 5. Hydrogen formation during CH_4–TPSR (legends same as in Fig. 3).

for the nickel doped sample (Mo–Ni), only a peak at 910 K was formed.

CO formation versus temperature is shown in Fig. 3B. There were two peaks, small one at 859 and the other within the temperature range from 959 to 1018 K, for the sample Mo. The intensity of the latter was so strong that it exceeded the detectable scope of the instrument. For the sample Mo–K, there were a shoulder peak at 938 K, and a strong peak at 1040 K. As for the sample Mo–Cu, there was a very small peak at 851 K, and a strong peak at 966 K, whereas there was a strong peak at 913 K for the sample Mo–Ni, and the signal at 850 K was so small that it cannot be taken a as peak.

The water formation versus temperature is shown in Fig. 4. For sample Mo, the formation of water was started at ca. 755 K, a band of water formation was finished at ca. 936 K, it followed a very strong peak within temperature range from 992 to 1008 K. For sample Mo–Cu, there were two peaks, one at 890 and the other at 964 K. For sample Mo–K, there were also two peaks, one at 936 and the other at 1048 K while for the sample Mo–Ni, there was a strong asymmetric peak at 918 K.

The formation of hydrogen versus temperature is shown in Fig. 5. It can be found that the hydrogen was once formed; it increased so fast that it exceeded the detectable scope of the instrument. However, as shown in Fig. 5, the temperature (T_M) at which the signal corresponding to the hydrogen formation exceeded the detectable scope was different for different samples, 945, 949, 989 and 910 K for sample Mo, Mo–Cu, Mo–K and Mo–Ni, respectively.

3.3. Characterization by XRD

The XRD patterns of the passivated carbide catalysts postcatalysis for 2 h are shown in Fig. 6. The presence of diffraction peaks at $2\theta = 34.4$, 38.0, 39.4, 61.6 and 69.5° indicated that molybdenum carbide modified or unmodified existed in the form of β-Mo_2C (hcp) according to references [3,12,13]. The diffraction peaks at $2\theta = 26.1$, 37.0, 52.1° showed the appearance of MoO_2 according to JCPDS 32-0671. The peak at 59.9° may be attributed to MoO_3 (JCPDS 47-1320) and the peak at 66.8° to Al_2O_3. These results showed that there were relatively less MoO_2 formed over sample Mo–Ni; and MoO_3 was possibly formed over sample Mo–K.

Table 1
BET specific area of the passivated carbide catalyst

Sample	Specific area (m^2/g catalyst)	Postcatalysis[a]
Mo	100.4	86.2
Mo–Ni	101.3	95.4
Mo–Cu	97.2	83.1
Mo–K	66.0	–

[a] The catalysts were used under the conditions same as Fig. 1.

3.4. Measurements of BET specific areas

The results of BET specific areas are summarized in Table 1. There was a decrease of BET specific area between pre- and postcatalysis for all samples. Among these samples, the decrease of BET specific area was larger for sample Mo–Cu, less for sample Mo–Ni postcatalysis for 2 h.

4. Discussion

The effect of secondary metals on Mo_2C/Al_2O_3 catalyst for the POM to syngas is clearly shown in Figs. 1 and 2.

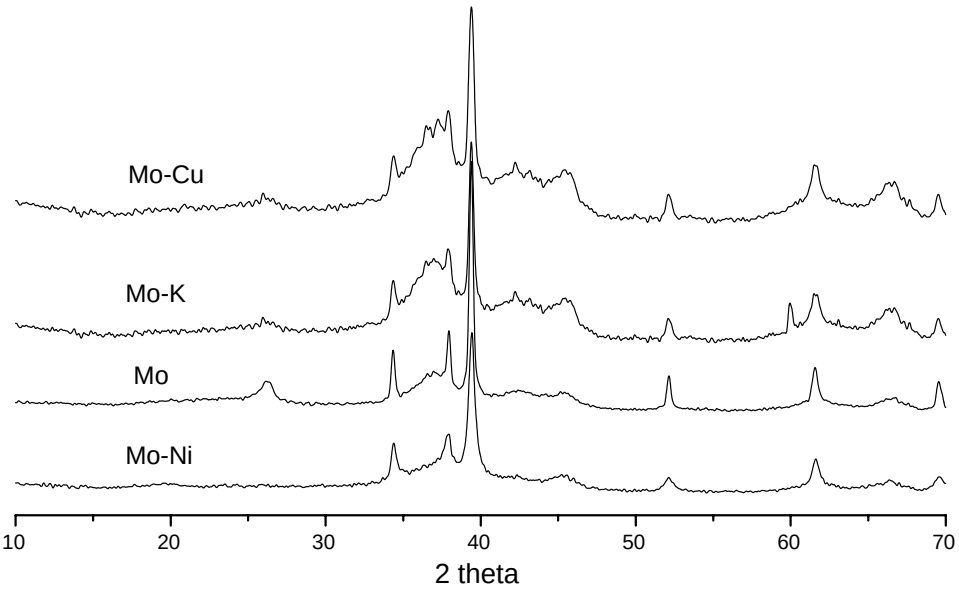

Fig. 6. XRD patterns of different samples (legends same as in Fig. 1).

Although nickel is also active for the POM to syngas, as shown in Fig. 1, Ni/Al_2O_3 catalyst deactivated rapidly due to it low loading (0.5 wt.%). When Mo_2C/Al_2O_3 catalyst was doped with nickel, the doped catalyst exhibited high methane conversion, even higher than the sum of that of corresponding Mo_2C/Al_2O_3 and that of Ni/Al_2O_3 after 1 h run. This indicated that there was a synergism between molybdenum carbide and nickel, besides their individual roles. The addition of potassium resulted in the drastic decrease of methane conversion, S_{CO} and S_H. However, it was interesting that the addition of copper promoted the methane conversion, S_{CO} and S_H at initial stage (for about 1 h), while lowered the methane conversion, S_{CO} and S_H afterwards.

As mentioned above, the deactivation of carbide catalyst under the existence of oxygen-containing species was mainly ascribed to its transformation into dioxide. Thus, the measurements of CH_4–TPSR with oxide precursors were carried out in other to investigate the effect of added metals on the carburization of molybdenum oxide. Although there are many routes for the carburization of molybdenum trioxide, among them, the key step is the reaction of molybdenum oxide with carbon-containing material [13], such as methane, ethane and butane, etc.

There are many factors, such support, loading, coarseness of surface, sample size, following rate of reducing agent and the rate of ramped temperature can affect the reduction of molybdenum oxide by hydrogen [14–17]. These factors should also affect the reduction of molybdenum oxide by methane. These are usually two peaks formed in the profile of H_2–TPSR for MoO_3 supported or unsupported [14,16,18,19], the peak at lower temperature corresponding to the reduction of MoO_3 to MoO_2, and the other, the reduction of MoO_2 to suboxide, even to metal. As shown in Figs. 3–5, there are also two peaks formed in the curves of CH_4–TPSR for all samples. In view of this, there is a similarity between the reduction of molybdenum oxide by hydrogen and by methane.

As shown in Figs. 3 and 4, the main products, CO, CO_2 and H_2O, resulted from the MoO_3 reduced by methane, was detected during CH_4–TPSR, though there should be also other products according to the reference [20]. Judging by the peak temperature (T_M) at which product formation is beyond the detectable scope of instrument, the addition of nickel or copper led to T_M shifting to lower temperature, while the addition of potassium led to T_M shifting to higher temperature. In view of this, nickel exhibited stronger than copper, promotion to the reduction of molybdenum oxide from the value of T_M shift, whereas potassium showed inhibition.

The effect of secondary metals on the reduction of molybdenum oxide can be explained from two aspects. One is the effect on the crystalline and electronic structure of surface phases. As for this, it cannot be discussed in detail. However, this effect should be limited within domains because of its low content and high dispersion. The other is the effect on the activation of methane. In view of the chemisorption heat [21] and activation energy [22] of methane over crystalline nickel or copper, nickel is more active for the activation of methane than copper. As reported in reference [23], the alkali potassium can prevent the turnover of propane on the surface of molybdenum oxide. In addition, potassium can strengthen the bonding of Mo–O in MoO_3 phase; weaken the intensity of Lewis acidic sites such as Mo^{6+}. These will result in the increase of activation energy of C–H [23]. Cu_2O is also of basicity, but weaker than K_2O. Hydrogen is highly mobile over the nickel species [24]. The nickel or copper ion can polarize the Mo–O bond under the reaction condition. All these factors led to the promotion of doped metals on the methane reduction of MoO_3 in the order; Ni > Cu > K. In fact, potassium is unfavorable to the reduction of MoO_3.

The oxygen in MoO_3 can be divided in two kinds; one is situated at end and binding with one Mo atom (O_a), the other is bridged with two Mo atoms (O_b). The bonding of O_a is relatively strong, while the bonding of O_b is loosely [25]. When MoO_3 is reduced with methane, O_b is easily to capture the H atoms resulted from the dissociation of methane to form HO_b group and HO_b is easily to be desorbed in the form of water. In this sense, desorption of the oxygen-containing species, e.g. CO, CO_2 and H_2O, should occur at different temperature, this is to say that there should be two peaks formed in the patterns of CH_4–TPSR. In fact, as shown in Figs. 3 and 4, there were two peaks in most cases. However, it is difficult to determine the relationship between O_a, O_b and the peaks in Figs. 3 and 4.

In the course of CH_4–TPSR, the dihydrogen was formed when temperature was elevated to some extent, particularly, a great amount of dihydrogen formed at T_M (Fig. 5). In generally, at these T_M, the pyrolysis of methane cannot occur. This means that the hydrogen formation, as shown in Fig. 5, should be ascribed to catalytic decomposition. The difference of this catalysis stemmed from two aspects: the intrinsic activity of catalytic centers and the components of surface phases, namely, carburization degree, of samples. Judging by the T_M in Fig. 5, nickel showed stronger promotion than copper, whereas the addition of copper hardly promoted hydrogen formation during the CH_4–TPSR. However, the addition of potassium prevented dihydrogen from being formed. If methane is to be decomposed, it must be activated. In this sense, the promotion to hydrogen formation is attributed to the influence on the capacity to activate methane. Thus, it can be concluded that nickel is of greater promotion to the activation of methane than copper; whilst the addition of potassium prevents the activation of methane over the surface of K doped sample.

In the view of formation of oxycarbide under the existence of the mixture of hydrogen and hydrocarbon [26], the hydrogen is responsible for the removing the oxygen to produce vacancies, while the carbon resulted from the dissociation of hydrocarbon is responsible for the carburization, namely, these vacancies occupied by carbon. According to the mechanism of the formation of carbide [13], the carbide is the result of oxygen in oxide completely replaced by the

carbon, while the oxycarbide is the medium product of carburization. Of course, there are corresponding changes of crystal lattice with this replacement.

During the CH_4–TPSR, oxygen is continuously removed with the elevated temperature. There are two routes for carbon resulted from the dissociation of methane to react: one is to bond oxygen atoms in surface phases, which results in the formation of carbon oxide; the other is to take the place of vacancies originated from the removed oxygen atoms, which results in the formation of oxycarbide, even of carbide at last [13,26]. Although it is very difficult to determine accurately the temperature at which the oxycarbide or carbide is formed, it is sure of the formation of oxycarbide during CH_4–TPSR. Judging from the profiles of hydrogen formation versus temperature in Fig. 5, it can be concluded that oxycarbide is very active for the activation of methane. As for the different T_M in Fig. 5, it may result from the role of added metal and/or surface phases, oxcarbide.

According to the mechanism of carbide formation [13,26], any factor which is favorable to the reduction of MoO_3 favors the carburization. Therefore, nickel is favorable to the carburization of MoO_3, copper is of a little promotion, whereas potassium is unfavorable to the carburization because of the reasons mentioned above. This promotion of nickel is similar to that of cobalt [27]. The role of potassium is associated with its inhibition of methane being absorbed on nickel [28] and the formation of deposited carbon [29]. In the course of carburization, the specific area is generally increased with elevated carburization degree [13]. From the data listed in Table 1, the specific area is in agreement with the promotion to the carburization, though this margin is small. When carburized, there is penetration of carbon atoms into and diffusion of oxygen atoms outside, the crystal lattice, which will leads to collapse of a portion of lattices due to the difference of atom size. This collapse will result in more and smaller particles formed, at same time, more surface defects, which is usually regarded as catalytic centers, are formed. With elevated carburization degree, there is higher active site density over the sample, just as described in reference [30]: higher carburization degree, more noble metal-like behaviors.

In accordance with the essential interpretation of the catalysis of carbide [31,32], the occupation of d-orbital of metal atoms is of great importance. Ni^{2+} generally shows electron donation [33]. This electronic interaction between nickel and molybdenum will result in the increase of d-orbital occupation of molybdenum atoms, which further increases the intrinsic activity. Theoretically, potassium will behave similar to nickel, but this electronic promotion is possible to be counteracted by other factors. As for copper, it shows electronic promotion when its oxidation state is less than $+1$ because it has relatively easily lost valent electron; when its oxidation state is no less than $+1$, it shows electron withdraw due to its tendency to form a d^{10}-electron structure, and at this time, it decreases the intrinsic activity of molybdenum carbide.

It should be noted at first that the pure carbide phases cannot exist. There are two reasons for this: one is the oxygen is very difficult to be removed [12,34]; the other is that carbide must be transformed into oxycarbide or oxide, at least, partly, due to the existence of oxygen. When we return to the effect of secondary metals on the performance of the POM to syngas, the promotion of nickel is easily understood. This promotion mainly resulted from two aspects: the promotion to intrinsic activity and to the active site density of catalyst. Firstly, as mentioned above, the interaction of d-electron resulted in the increase of intrinsic activity of molybdenum carbide. Secondly, the promotion of nickel to the carburization resulted in more active phases with higher active site density formed. It was important that this promotion also remained effective in the reaction of POM to sygas. Therefore, it led to more active phases being held in the course of the POM, which improved stability of catalytic performance. At same time, the capacity to activate methane was elevated. This promotion was also affirmed by the XRD result as shown in Fig. 6, obviously, there was less MoO_2 phases formed over nickel doped sample postcatalysis. Finally, as summarized in Table 1, the specific area decreased relatively slowly, which may be partly attributed to the improved sintering resistance of nickel; partly to the carbon deposition. At the initial stage of the POM to syngas, copper existed in metallic state because it was treated with the mixture of hydrogen and methane for hours, which promoted the intrinsic activity of molybdenum carbide or oxycarbide. Furthermore, it also promoted the carburization of MoO_2, especially in the course of the POM to syngas, which resulted in more active phases being held. Therefore, the addition of copper promoted the methane conversion and selectivity to CO and H_2 at the initial stage. With the POM reaction in progress, its oxidation state was increased due to the existence of oxygen. After this increase, it was of no electronic promotion to carbide or oxycarbide, even it turned unfavorable to the intrinsic activity. Of course, the promotion to the carburization always existed, but only to limited extent. In addition, copper-containing species is easily to sinter [35], this can be also concluded from the margin of specific area between pre- and postcatalysis listed in Table 1. When copper ion became Cu^{2+}, it catalyze the products such as, CO or H_2, to be deeply oxidized [36], which led to the decrease of S_{CO} and S_H, as shown in Fig. 2. All these factor made copper be unfavorable to the POM to syngas at latter stage. As for potassium doped catalyst, on one side, potassium prevented molybdenum oxide from carburization, namely, it was favorable to the transformation of carbide into oxide. As shown in Fig. 6, even there was MoO_3 formed over the K doped catalyst. Under the condition of the POM, this action was particularly detrimental to the methane conversion and selectivity to CO and H_2. With the POM progressing, the transformation of carbide into oxide resulted in active phases becoming less and less. On the other hand, the addition of potassium promoted the sintering of catalyst, this conclusion can be

obtained from the data summarized in Table 1. Therefore, it is natural for the potassium doped catalyst to deactivate rapidly.

5. Conclusions

It can be concluded from the above discussion that:

1. Nickel, even though a little, can promote the reduction, further the carburization, of MoO_3 by methane, which results in greater specific area of catalyst. This promotion leads to more active phases, carbide or oxycarbide, being held in the course of the POM to syngas, which stabilizes the catalytic performance. Nickel can activate methane, and it can also promote the activation of methane over the surface of molybdenum carbide, which is favorable to the POM shifting to thermodynamic equilibriums. All these factors are responsible for the high conversion of methane, high selectivity toward CO and H_2 and high stability for nickel doped catalyst.
2. The addition of potassium is unfavorable to the reduction of MoO_3 by methane, and thus it is unfavorable to the carburization of MoO_3. Potassium can accelerate the sintering of carbide catalyst. Therefore, the potassium doped carbide catalyst is of lower specific area. These impair the stability of carbide catalyst. The addition of potassium can also prevent the activation of methane over the surface of molybdenum carbide. Therefore, high yield of syngas and highly stable catalytic performance cannot be obtained over the potassium doped molybdenum carbide catalyst.
3. The addition of copper can promote the reduction of MoO_3 by methane to some extent, which is favorable to the carburization. Copper with low oxidation state (<1) can promote the methane conversion and yield of CO and H_2. However, under the existence of oxygen, the low valent copper can be oxidized, while the Cu^{2+} is active for the total oxidation of methane. Copper can also accelerate the sintering of carbide catalyst. These reasons are responsible for the promotion to the POM to syngas at initial reaction stage, what follows is that the conversion of methane and selectivity to CO and H_2 drop quickly.

Acknowledgements

This work has been financially supported by the Foundation of National Fundamental Research & Development. We are grateful to Madam Li and Madam He, our colleagues, for the BET specific area and XRD measurements, respectively.

References

[1] A.P.E. York, J.B. Claridge, A.J. Brungs, S.C. Tsang, M.L.H. Green, J. Chem. Soc. Chem. Commun. (1997) 39.
[2] A.P.E. York, J.B. Claridge, A.J. Brungs, C. Márquez-Alvarez, S.C. Tsang, M.L.H. Green, Stud. Surf. Sci. Catal. 110 (1997) 711.
[3] J.B. Claridge, A.P.E. York, C. Márquez-Alvarez, A.J. Brungs, J. Sloan, S.C. Tsang, M.L.H. Green, J. Catal. 180 (1998) 85.
[4] T.C. Xiao, H.T. Wang, A.P.E. York, M.L.H. Green, Catal. Lett. 83 (2002) 241.
[5] A.J. Brungs, A.P.E. York, J.B. Claridge, C. Márquez-Alvarez, M.L.H. Green, Catal. Lett. 70 (2000) 117.
[6] A.J. Brungs, A.P.E. York, M.L.H. Green, Catal. Lett. 57 (1999) 65.
[7] M. Tsuji, T. Miyao, S. Naito, Catal. Lett. 69 (2000) 195.
[8] J. Sehested, C.H.J. Jacobsen, S. Rokni, J.R. Rostrup-Nielsen, J. Catal. 201 (2001) 206.
[9] J.L. Zeng, Z.T. Xiong, H.B. Zhang, G.D. Lin, K.R. Tsai, Catal. Lett. 53 (1998) 119.
[10] J.L. Zeng, Z.T. Xiong, G.D. Lin, L. Yu, H.B. Zhang, Acta Phys. Chem. Sin. 14 (1998) 394.
[11] J.S. Lee, S.T. Oyama, M. Boudart, J. Catal. 106 (1987) 125.
[12] K. Oshikawa, M. Nagai, S. Omi, J. Phys. Chem. B 105 (2001) 9124.
[13] A. Hanif, T.C. Xiao, A.P.E. York, J. Sloan, M.L.H. Green, Chem. Mater. 14 (2002) 1009.
[14] P. Arnoldy, J.C.M. De Jonge, J.A. Moulijn, J. Phys. Chem. 89 (1985) 4517.
[15] T. Ressler, R.E. Jentoft, J. Wienold, M.M. Gunter, O. Timpe, J. Phys. Chem. B 104 (2000) 6360.
[16] W.V. Schulmeyer, H.M. Ortner, Int. J. Refract. Met. Hard Mater. 20 (2002) 261.
[17] S. Li, W.B. Kim, J.S. Lee, Chem. Mater. 10 (1998) 1853.
[18] S. Damyanova, A. Spojakina, K. Jiratova, Appl. Catal. A: Gen. 125 (1995) 257.
[19] T. Ressler, O. Timpe, T. Neisius, J. Find, G. Mestl, M. Dieterle, R. Schlogl, J. Catal. 191 (2000) 75.
[20] X. Xu, F. Faglioni, W.A. Goddard III, J. Phys. Chem. A 106 (2002) 7171.
[21] C.W. Robert (Ed.), CRC Handbook of Chemistry and Physics, CRC Press, Boca Raton, 1985–1986, pp. F174–194.
[22] M.J. Hei, H.B. Chen, J. Yi, Y.J. Lin, Y.Z. Lin, G. Wei, D.W. Liao, Surf. Sci. 417 (1998) 82.
[23] K.D. Chen, S.B. Xie, A.T. Bell, E. Iglesia, J. Catal. 195 (2000) 244.
[24] S. Harris, R.R. Chianelli, J. Catal. 98 (1986) 17.
[25] K. Hermann, A. Michalak, M. Witko, Catal. Today 32 (1996) 321.
[26] P. Delporte, F. Meunier, C. Pham-Huu, P. Vennegues, M.J. Ledoux, Guille J. Catal. Today 23 (1995) 251.
[27] T.C. Xiao, A.P.E. York, H. Al-Megren, C.V. Williams, H.T. Wang, M.L.H. Green, J. Catal. 202 (2001) 100.
[28] H.S. Bengaard, I.B. Alstrup, I.B. Chorkendorff, S. Ullmann, J.R. Rostrup-Nielsen, J.K. Nørskov, J. Catal. 187 (1999) 238.
[29] T. Osaki, T. Mori, J. Catal. 204 (2001) 89.
[30] J.S. Choi, G. Bugli, G. Dj'ega-Mariadassou, J. Catal. 193 (2000) 238.
[31] R. Siegel, Semiconductors Insulators 5 (1979) 47.
[32] V. Heine, Phys. Rev. 153 (1967) 673.
[33] Y.V. Zubavichus, Y.L. Slovokhotov, P.J. Schilling, R.C. Tittsworth, A.S. Golub, G.A. Protzenko, Y.N. Novikov, Inorg. Chim. Acta 280 (1998) 211.
[34] C. Bouchy, C. Pham-Huu, B. Heinrich, C. Chaumont, M.J. Ledoux, J. Catal. 190 (2000) 92.
[35] M.V. Twigg, M.S. Spencer, Appl. Catal. A 212 (2001) 161.
[36] O.V. Komova, A.V. Simakov, V.A. Rogov, et al., J. Mol. Catal. A 161 (2000) 191.